RESEARCH   **Open Access**

Optimising Al$_2$O$_3$–water nanofluid

Ekene Onyiriuka[1*] ⓘ

Abstract

Background This study explores how nanofluids can be optimised to improve heat transfer in various applications. A genetic algorithm that finds the optimal parameter configuration to achieve the best performance is studied and applied. The research focuses on the critical factors of heat transfer coefficient and pressure drop, which determine the efficiency of nanofluid-based systems.

The main body of the abstract The methodology involves artificial intelligence and multi-objective optimisation techniques. Results show that pressure drop and heat transfer coefficient have an inverse relationship. The study provides a range of optimal values for nanofluid temperature, particle size, and volume fraction.

Results The results show that the temperature, particle size, and volume fraction should be high. Another variation will be small particle size and small volume fractions with fluid temperature around 80 ℃. The analysis yielded the following configuration with the optimal PEC. Temperature (^{o}C), particle size (nm), volume fraction (%), heat transfer coefficient (kW/m^{2}K), pressure drop (Pas), and PEC were 82.6 ℃, 175.26 nm, 4.75%, 792.49 kW/m^{2}K, 29.94 Pas, and 5.01.

Conclusions The research highlights the potential of Al$_2$O$_3$–water nanofluids to maintain pressure drop and enhance heat transfer. It contributes to understanding nanofluid optimisation and provides practical insights for designing and selecting nanofluid systems that enhance heat transfer.

Keywords Nanofluids, Enhancement, Heat transfer, Optimisation, Genetic algorithm, Multi-objective optimisation, Al$_2$O$_3$–water nanofluids

Background

Numerous researchers have recognised the enhanced thermal characteristics of nanofluids. However, the optimal selection of parameters for obtaining the best nanofluids remains to be determined. This paper presents these research queries and endeavours to offer feasible solutions (Hojjat 2022). A study was conducted to determine the optimal conditions for heat transfer in rectangular ducts using nanofluids. The researchers found that an optimal geometry, nanofluid, and flow conditions are necessary for efficient heat transfer. They used numerical simulations and artificial neural networks to model heat transfer coefficient and pressure drop. They used the NAGA-11 multi-objective optimisation algorithm to find the optimal aspect ratio for rectangular ducts with nanofluids. The researchers also applied TOPSIS and LINMAP, a linear programming-based method that maps decision criteria and preferences to a scale. Overall, they obtained an optimal solution at 2.28% volume fraction, a Reynolds number of 400, and an aspect ratio of 6 while highlighting the effects of concentration and aspect ratio on heat transfer and pressure drop. In their study, they showed the Pareto fronts obtained from the multi-objective optimisation of the problem, showing all the non-dominated solutions. Property computations were carried out using formulas and correlations. The MLP-ANN algorithm was applied with a data split ratio of 70:10:20—train:validation:test, with inputs as volume fraction (%), aspect ratio (AR), and Reynolds number. The algorithm had three hidden layers with five neurons with tansig as the activation function, and the output layer was the purelin function. The Levenberg–Marquardt

*Correspondence:
Ekene Onyiriuka
mnejo@leeds.ac.uk
[1] School of Mechanical Engineering, University of Leeds, Leeds LS2 9JT, UK

algorithm was used to train the algorithm, and 100 data points not seen in the training were generated. Symmetry was applied, and flow regime was the 400–2200 Reynolds number range, considering up to 5% volume fraction of the Al_2O_3/water. A hydraulic diameter of 0.01 was applied in all ducts (Azmi et al. 2017). The significance and potential of nanofluids in improving the efficiency and mechanical performance of refrigeration systems were emphasised. A brief history of refrigerant phases was also highlighted, particularly the introduction of fluorocarbon refrigerants in 1930 due to safety and durability concerns. These refrigerants aim to eliminate toxic compounds and flammable properties. Optimising nanofluids performance in heat exchangers was found to lead to more energy savings and efficient system operation. Adding nanoparticles to refrigerant and lubricant oil enhanced the heat transfer coefficient in heat exchangers, resulting in increased energy savings. Using a refrigerant and nanolubricant mixture was crucial to achieving better performance in vapour compression of refrigeration systems for specific applications. A 21% energy saving was recorded with the use of ZnO/R152a refrigerant nanolubricant. Due to its potential, there is a drive to use nanorefrigerants in various applications (Kamsuwan et al. 2023). The PEC measures the heat transfer coefficient to pressure drop ratio between nanofluid and water. When PEC is greater than 1, it indicates that the nanofluid can achieve the same heat transfer at a lower pumping cost.

A study was conducted to investigate the behaviour of nanofluid flow and convective heat transfer within microtubes. The microtubes were subjected to constant wall temperature and constant heat flux boundary conditions. The analysis used a multiphase Eulerian–Lagrangian method and focused on assessing the effects of three key parameters: the Peclet number (ranging from 175 to 3500), nanoparticle volume fraction (varying from 0.1% to 1.0%), and nanoparticle diameter (ranging from 40 to 130 nm) on the thermal characteristics of Al_2O_3–water nanofluid flow through a microtube, specifically noting the entry region effects (Ma et al. 2023).

The investigation revealed several important insights. The entry effects of Reynolds number on the apparent friction factor and the axial heat conduction impact on the Nusselt number had to be considered. The entrance region characteristics had a more dominant role in determining the pressure drop and thermal performance compared to the effects of nanoparticle concentration and size. However, as the dimensionless axial distance increased, the influence of the entrance region gradually diminished, and the impact of nanoparticle concentration and size became more pronounced in the flow and heat transfer results. Nanoparticles had an earlier and

greater impact on the thermal performance of the nanofluids than on flow resistance (Ma et al. 2023).

The performance evaluation demonstrated that nanofluids in the entry region showed enhanced heat transfer and economic feasibility. For instance, when the Peclet number was set at 175, Al_2O_3–water nanofluids with particle concentrations of 0.1%, 0.2%, 0.5%, and 1% showed substantial increases in the performance evaluation criterion (PEC) under both constant heat flux and constant wall temperature conditions at a dimensionless axial distance of $x^* = 0.01$, compared to deionised water. Under constant heat flux conditions, the PEC improved by 104.0%, 103.1%, 113.8%, and 128.5%, respectively. Under constant wall temperature conditions, the PEC improved by 74.6%, 77.2%, 85.6%, and 102.5%, respectively, compared to deionised water (Ma et al. 2023).

The researchers aimed to create a parabolic trough collector (PTC) that had an insulator roof and an off-centre absorber tube, using nanofluid. They analysed the nanofluid using two different models, single-phase and two-phase mixture (TPM and SPM), which contained SiC nanoparticles with diameters ranging from 16 to 90 nm and varying volume fractions (0%–4%), mixed with water and EG–water. The study looked at how using TPM and SPM affected the fluid dynamics and heat transfer within the absorber tube (Arani and Monfaredi 2023).

The investigation showed some significant findings. Firstly, using TPM resulted in higher values for parameters such as pressure drop (3%), Nusselt number (5%), friction factor (3%), energy efficiency (3%), and the performance evaluation criteria (PEC) (3%) for both the novel PTC design and the conventional PTC arrangement, compared to SPM. Additionally, the novel PTC design, when using TPM, showed significantly improved Nusselt numbers (25%), energy efficiency (30%), and PEC (50%) (Arani and Monfaredi 2023).

Moreover, when TPM was employed, the temperature distribution within the absorber tube and the heat transfer fluid region was found to be higher than when using SPM. The highest PEC was achieved for SiC/EG–water and EG–water nanofluids, reaching 1.67 and 1.70, respectively, in a sinusoidal-wavy minichannel with a nanoparticle volume fraction of 4%, nanoparticle diameter of 90 nm, and a Reynolds number of 15,001.3. It was also noted that EG–water, as the base fluid with a nanoparticle diameter of 90 nm, demonstrated superior energy efficiency compared to pure water (Arani and Monfaredi 2023).

In Baro et al. (2023), the optimisation of a nanofluid-based direct absorption solar collector (NDASC) was explored to achieve maximum thermal efficiency and temperature increase. Computational fluid dynamics was used to solve equations for mass, momentum, energy balance, and wavelength-dependent radiative transport

within a three-dimensional NDASC model. The goal was to maximise thermal efficiency and temperature rise while adhering to a constraint on the maximum temperature rise for low-temperature NDASC. To achieve this, various computational intelligence techniques such as multi-objective genetic algorithms (MOGA), multi-objective particle swarm optimisation (MOPSO), and multi-objective differential evolution (MODE) were employed. The key decision variables that significantly impact the NDASC thermal performance include collector geometry (length, width, and height), nanoparticle properties (volume fraction), and collector operational parameters (mass flow rate and fluid inlet temperature). MOPSO was found to be the most effective optimisation algorithm in terms of objective function values and solution convergence. Pareto solutions were obtained, and sensitivity analysis was conducted using the corner point solutions from the Pareto front determined by MOPSO. The results showed that NDASC thermal efficiency ranges from 59.9% to 98.4%, while temperature rise varies between 7.81 K and 71.93 K, subject to the specified constraint. This research contributes to the development of compact and efficient NDASC designs capable of achieving the required thermal efficiency and temperature rise for a wide array of low-temperature applications in residential and industrial settings (Baro et al. 2023).

In their article (Bhatti and Ellahi 2023), the authors conducted a numerical investigation of the flow of a non-Darcian nanofluid over an elastic surface that can stretch. They assumed that the fluid is viscous, electrically conductive, and flows through a porous material. The study considered various factors such as heat radiation, Brownian motion, and viscous dissipation in this flow configuration. The boundary conditions included slip velocity and thermal slip. The mathematical modelling used similarity variables, resulting in a set of nonlinearly coupled differential equations. To solve these equations, the authors used the Keller-box approach in combination with a finite difference scheme. All numerical simulations were carried out using MATLAB software, and the results were presented, giving insights into key physical parameters such as the local Sherwood number, skin friction coefficient, and Nusselt number (Bhatti and Ellahi 2023).

In their study (Dehghan et al. 2023), the researchers examined how an inclined step and different obstacle arrangements affected heat transfer in a microchannel with graphene oxide nanofluid. They used a numerical model with ANSYS Fluent 19.0 software and conducted simulations to improve forced convection heat transfer. The investigation focused on Reynolds numbers (1, 50, and 100), nanofluid nanoparticle volume fractions (0, 0.02, and 0.04), and the presence and location of triangular obstacles (Dehghan et al. 2023).

The results show that placing triangular obstacles at the top of the first step, combined with a nanoparticle volume fraction of 4% and Reynolds numbers of 50 and 1, led to significant improvements in heat transfer. Compared to pure water, there was a maximum increase of 12.7% in the Nusselt number and a 12.3% rise in the heat transfer coefficient. However, this improvement also resulted in higher pressure drop and friction factors, which were affected by the presence and location of the obstacles (Dehghan et al. 2023).

In Hojjat (2022), it is important to note that only one type of flow geometry was considered. The implications of validating only with cylindrical pipe flow instead of rectangular pipe were noted. It was observed that symmetry would not work with cylindrical pipe flow, whereas it would be valid in rectangular flow. It is important to mention that the symmetry assumption is not valid in pipe flow due to the elemental differences between flow field in a circular pipe and that in a rectangular duct. While the flow in a rectangular duct is symmetrical with respect to the middle plane, the velocity profile is symmetric, and the pressure distribution is uniform along the length but not across the circumference, the flow in a circular pipe is non-symmetric. Consequently, the velocity profile is parabolic due to the no-slip condition at the pipe wall, and the pressure distribution decreases along the length due to frictionless losses, but it is uniform across the circumference. There is also a secondary flow component present in a circular pipe due to the continuous helical motion of fluid flow around the circumference of the pipe, which significantly affects the overall flow behaviour and cannot be accounted for assuming symmetry. To simplify the problem, steady states, fully developed flow, and constant fluid properties assumptions should be applied. The axisymmetric assumptions are also useful, assuming that the flow field is symmetric about the axis of rotation. However, it is not valid for large variation in cross-section and complex geometry.

In Rudyak and Minakov (2018) this study, the authors outlined several issues bordering on the thermophysical properties of nanofluids. This included how each feature affects heat and the heat transfer of nanofluids.

The heat transfer coefficient was also studied in a heat stainless steel tube of 6-mm diameter and 1 m. The heat transfer coefficient of nanofluids increased with the particle concentration; for 1%, a 40% increase and, for 2%, a 100% increase were noted. It was pointed out that this increase was almost proportional to the volume concentration of nanoparticles. At low Reynolds numbers, where laminar flow conditions are prevalent, an increase in thermal conductivity leads to an almost linear increase in the heat transfer coefficient. It was also noted that there was an optimal point for the heat transfer coefficient regarding the particle size. They explained that it was because, in turbulent flow conditions, heat transfers of nanofluids

depend on two factors; apart from its thermal conductivity, it also depends on the viscosity, which is the parameter that influences the heat transfer negatively, such that if the viscosity increases more than the thermal conductivity for a particular nanoparticle size, the heat transfer coefficient will decrease. Therefore, there will be an optimal nanoparticle size for different nanofluids to have any increasing gains in heat transfer for nanofluids compared to their base fluid. This study attributed this binding effect in the heat transfer field to the nanoparticle size, not any other parameter, like its concentration or material type. They also stated that it was best to avoid similarity criteria, such as the Prandtl number, Pr, as it is not uniquely tied to the particular nanofluid of interest but can refer to another nanofluid not explicitly considered.

Numerous researchers (Sridhara and Satapathy 2011; Nazififard et al. 2012; Usman et al. 2022; Fadodun et al. 2022) have conducted studies using different approaches to achieve optimal heat transfer and pressure drop. However, this study distinguishes itself by identifying the potential design parameters and design points. Additionally, it provides insight on the features to consider during the development, application, and optimisation of nanofluids, using an example of aluminium oxide–water nanofluid.

Methods

For this study, we utilised the following methodology:

We utilised a circular pipe that measured 0.5 m in length and had an inner diameter of 4 mm. To maintain consistency, we applied a constant wall temperature of 50 °C and an inlet velocity of 0.1 m/s.

Nanofluids thermal conductivity and viscosity were modelled using machine learning. For thermal conductivity, a trilayer neural network was chosen with three fully connected layers. The first, second, and third layers had a size of 10. The activation used was ReLU (rectified linear unit), and there was no regularisation strength applied. The data were standardised. The selected variables in the study had distinct statistical characteristics and varied values. These variables included the temperature of the nanofluid, particle size, volume fraction, nanoparticle thermal conductivity, nanoparticle melting point, base fluid kinematic viscosity, and base fluid viscosity. The models validation results showed an RMSE of 1.83, MSE of 3.34, RSQUARED of 0.94, and MAE of 1.23. The test results showed an MAE of 0.99, MSE of 2.14, RMSE of 1.46, and RSQUARED of 0.97 (Onyiriuka 2023a).

For viscosity, a custom Gaussian process regression with signal standard deviation sets to 0.20121 and optimises numeric parameters. The study examined various factors that had unique statistical characteristics. These variables included the temperature of the nanofluid, particle size, volume fraction, nanoparticle specific heat,

nanoparticle dielectric constant, base fluid density, and base fluid specific heat capacity. On the validation set, the model had the following result an RMSE of 0.0157, MSE of 0.0005, RSQUARED of 0.9941, and MAE of 0.0146. Furthermore, the test results indicated an MAE of 0.99, MSE of 0.0004, RMSE of 0.0211, and RSQUARED of 0.9924 (Onyiriuka 2023b).

Afterwards, Nusselt's number was calculated using the Sieder–Tate correlation, assuming a constant wall temperature boundary condition of 50 °C where water viscosity is 0.000282 Pas.

Sieder–Tate equation (Eq. 1)

$$Nu_{nf} = 1.86 * (Re_{nf})^{\frac{1}{3}} * (Pr_{nf})^{\frac{1}{3}} * \left(\frac{D_h}{L}\right)^{\frac{1}{3}} \left(\frac{\mu_{nf}}{\mu_{nf@T_{wall}}}\right)^{0.14} \tag{1}$$

The heat transfer coefficient is calculated using an equation based on the Nusselt number (Eq. 2).

$$Nu = \frac{h * D}{k} \tag{2}$$

The calculation of the Darcy friction factor (Eq. 3) was carried out.

$$f_d = \frac{64}{Re} \tag{3}$$

To calculate the pressure drop in the pipe, we use the Darcy friction factor in Eq. 4.

$$\Delta p = \frac{L * f_d * \rho}{2 * D_h} * v^2 \tag{4}$$

To calculate the Reynolds number, follow this formula (Eq. 5):

$$Re = \frac{\rho * v * D_h}{\mu} \tag{5}$$

The Prandtl number can be determined using Eq. 6.

$$Pr = \frac{cp * \mu}{k} \tag{6}$$

The genetic algorithm was applied to carry out a multi-objective optimisation. It maximised the heat transfer coefficient and minimised the pressure drop.

A search and optimisation algorithm based on natural selection and evolution, the genetic algorithm is commonly used for solving complex optimisation problems (Li et al. 2023; Zhang et al. 2023; Pan et al. 2023; Liu et al. 2023; Nguyen et al. 2023). It is a popular optimisation algorithm and used by prominent researchers (Li et al. 2023). The algorithm generates a population of potential solutions represented as individuals or chromosomes. Each chromosome

contains a candidate solution to the problem. The algorithm then evolves the population over multiple generations to find the best solution. The main steps of a genetic algorithm are as follows (Li et al. 2023): 1. Initialisation: A population of random solutions is created, with each solution represented as a chromosome. 2. Fitness evaluation: An objective function is used to assess the fitness of each chromosome. This function measures how well each chromosome solves the problem and determines the criteria for selecting the best solutions. 3. Selection: A subset of chromosomes with higher fitness values is chosen for reproduction. The selection process is often based on a fitness proportionate scheme, where fitter individuals are more likely to be selected. 4. Reproduction: The selected chromosomes create offspring through genetic operators such as crossover and mutation. 5. Replacement: The offspring replaces some less-fit individuals, keeping the overall population size constant. This allows the algorithm to explore new areas of the solution space. 6. Termination: The algorithm continues evolving the population through multiple generations until a termination criterion is met. This could be a maximum number of generations, a desired fitness level, or a predefined convergence threshold. By applying selection, reproduction, and replacement steps, the genetic algorithm explores the solution space, gradually improving the quality of solutions over generations. The algorithm tends to converge towards an optimal or near-optimal solution.

Genetic algorithms are particularly useful for solving complex optimisation problems with large search spaces, multiple objectives, or nonlinear constraints. They have been successfully applied in various domains, including engineering, finance, biology, and artificial intelligence. Genetic algorithms provide a powerful and flexible approach for finding approximate solutions to challenging optimisation problems. By mimicking the process of natural evolution, they iteratively improve solutions over time.

This study utilised a genetic algorithm with a population of 100 individuals over 50 generations. The Pareto plots were computed. The PEC values were computed for the local Pareto optimal using Eq. 7 (El-Shafay et al. 2023; Said et al. 2021).

$$\text{PEC} = \frac{\frac{Nu_{\text{nf}}}{Nu_{\text{bf}}}}{\left(\frac{f_{\text{d,nf}}}{f_{\text{d,bf}}}\right)^{1/3}} \tag{7}$$

Results

Discussion
In Fig. 1, the Pareto plots indicate an inverse relationship between the pressure drop and heat transfer coefficient. The curve's steepness demonstrates the strength of this correlation. These plots display the optimal trade-off
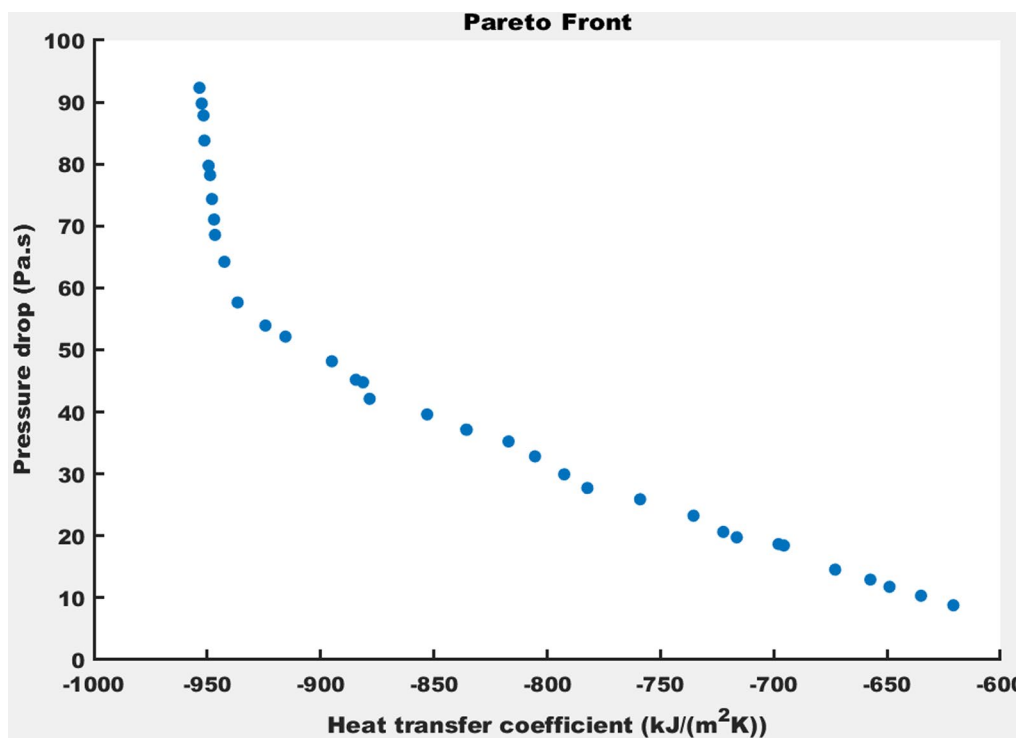

Fig. 1 Pareto fronts

solutions where objective improvement in heat transfer cannot occur without compromising performance in pressure drop function. Table 1 presents a range of values that offer many options for selecting the optimal nanofluid for various needs. The data highlight the Al_2O_3–water nanofluids' potential for proper pressure drop maintenance while providing adequate heat transfer.

Table 1 shows that the temperature should be high, particle size should be high, and volume fraction should be high. Another variation will be small particle size and small volume fractions with fluid temperature around 80 °C. The analysis yielded the following configuration with the optimal PEC. Temperature (oC), particle size (nm), volume fraction (%), heat transfer coefficient (kW/m^2 K), pressure drop (Pas), and PEC were 82.6 °C, 175.26 nm, 4.75%, 792.49 kW/m^{2}K, 29.94 Pas, and 5.01.

It is important to note that the range of nanoparticle size in this study was set to be between 10 and 200 nm, a standard nanoparticle size range for nanofluids.

Table 1 The local optimal points along with their corresponding PEC

Temperature (°C)	Particle size (nm)	Volume fraction (%)	Heat transfer coefficient (kW/m^2 K)	Pressure drop (Pas)	PEC
82.6	175.26	4.75	792.49	29.94	5.01
84.5	30.13	1.56	835.48	37.15	4.75
83.2	12.92	2.45	884.43	45.17	4.51
84.5	12.89	3.31	895.01	48.15	4.44
69.7	11.09	5.00	946.59	68.56	4.14
84.3	13.32	4.52	924.34	53.92	4.31
79.3	175.98	4.82	805.37	32.84	4.91
77.0	176.18	4.93	817.05	35.26	4.83
84.0	186.95	0.89	620.76	8.79	6.58
83.3	183.64	1.29	648.93	11.77	6.21
82.7	13.70	1.74	878.34	42.14	4.56
83.4	181.68	1.84	672.92	14.55	5.94
83.3	183.48	2.99	716.35	19.76	5.55
74.6	11.85	4.96	942.44	64.22	4.18
58.1	11.21	5.00	948.74	78.22	4.07
82.4	181.08	4.06	758.99	25.91	5.21
84.0	11.75	4.02	915.50	52.13	4.35
83.3	182.24	4.64	782.25	27.73	5.09
81.8	11.35	4.81	936.60	57.65	4.25
81.3	173.25	2.04	697.90	18.67	5.66
81.9	14.38	2.17	881.26	44.76	4.52
84.0	180.95	1.01	635.03	10.34	6.38
46.1	12.12	4.97	951.64	87.86	4.00
83.3	177.57	1.32	657.36	12.94	6.10
84.5	30.13	1.56	835.72	37.16	4.75
56.2	11.23	4.99	949.41	79.73	4.06
66.7	11.28	4.99	946.99	71.05	4.12
83.9	25.26	1.82	852.96	39.62	4.66
80.5	174.16	1.89	695.55	18.45	5.68
62.7	11.16	4.99	947.90	74.35	4.09
79.9	184.40	3.16	735.43	23.26	5.36
82.9	183.46	3.10	722.29	20.64	5.49
51.3	11.23	5.00	951.25	83.81	4.03
43.7	12.41	4.98	952.44	89.79	3.99
40.7	13.00	4.99	953.44	92.32	3.97

Conclusions

This article delves into the optimisation of nanofluids to enhance heat transfer performance. The study uses a genetic algorithm to identify configurations of parameters that maximise the heat transfer coefficient while minimising pressure drop. The results show that pressure drop and heat transfer coefficient have an inverse relationship, highlighting the trade-off in nanofluid systems. Pareto plots demonstrate the options for selecting the optimal nanofluid based on specific needs and requirements. The study suggests that Al_2O_3–water nanofluids have promising performance in maintaining pressure drop while delivering efficient heat transfer. Optimal values for temperature, particle size, and volume fraction of nanofluids were identified, providing valuable insights for the design and selection of nanofluid systems. Using machine learning and multi-objective optimisation techniques proves effective in solving complex optimisation problems in nanofluids. This research contributes to understanding nanofluid optimisation and offers practical guidance for engineers and researchers involved in designing and developing efficient heat transfer systems. The findings can be applied to various applications, such as refrigeration systems and industrial heat exchangers, to improve energy efficiency and overall system performance. Further research can expand on this work by exploring additional parameters, more complex geometries, and flow conditions. Experimental validation of the optimal configurations obtained through the genetic algorithm would provide more confidence in the results and enable a more comprehensive understanding of nanofluid behaviour. Overall, this study advances the knowledge and application of nanofluids for enhanced heat transfer, paving the way for developing more efficient and sustainable thermal management systems in various industries and applications.

Abbreviations

C_p	Specific heat capacity (kg/kgK)
D_h	Hydraulic diameter (m)
f_D	Darcy friction factor
h	Heat transfer coefficient (W/m^2 K)
k	Thermal conductivity (W/mK)
L	Length (m)
MAE	Mean absolute error
MSE	Mean squared error
Nu	Nusselt number
Pr	Prandtl number
Re	Reynolds number
$ReLU$	Rectified linear unit
RMSE	Root-mean-squared error
RSQUARED	Coefficient of determination
Δp	Pressure drop (Pa)
PEC	Performance evaluation criteria
v	Velocity (m/s)

Greek letters

μ	*Viscosity* (Pas)
ρ	*Density* (kg/m^3)

Subscripts

Bf	Basefluid
Nf	Nanofluid
Wall	The geometry flow boundary

Availability of data and material

All data sources were referenced in the manuscript body.

Declarations

Ethics approval and consent to participate

Not applicable.

Consent for publication

Not applicable.

Competing interests

The author declares that there are no competing interests.

References

Arani AAA, Monfaredi F (2023) Nanofluid turbulent flow in parabolic trough collector: insulator roof, acentric absorber tube and SiC nanoparticles effects. Eng Anal Boundary Elem 156:160–174

Azmi W, Sharif M, Yusof T, Mamat R, Redhwan A (2017) Potential of nanorefrigerant and nanolubricant on energy saving in refrigeration system–A review. Renew Sustain Energy Rev 69:415–428

Baro RK, Kotecha P, Anandalakshmi R (2023) Multi-objective optimization of nanofluid-based direct absorption solar collector for low-temperature applications. J Build Eng 72:106258

Bhatti MM, Ellahi R (2023) Numerical investigation of non-Darcian nanofluid flow across a stretchy elastic medium with velocity and thermal slips. Numer Heat Transfer Part B Fund 83(5):323–343

Dehghan P, Keramat F, Mofarahi M, Lee C-H (2023) Computational fluid dynamic analysis of graphene oxide/water nanofluid heat transfer over a double backward-facing microchannel. J Taiwan Inst Chem Eng 145:104821

El-Shafay AS, Mohamed AM, Ağbulut Ü, Gad MS, El Maakoul A (2023) Investigation of the effect of magnetic field on the PEC and exergy of heat exchanger filled with two-phase hybrid nanofluid, equipped with an edged twisted tape. Eng Anal Bound Elements 148:153–164

Fadodun OG, Ewim DRE, Abolarin SM (2022) Investigation of turbulent entropy production rate with SWCNT/H2O nanofluid flowing in various inwardly corrugated pipes. Heat Transfer 51(8):7862–7889

Hojjat M (2022) Numerical simulation and multi-objective optimization of heat transfer of Al2O3/water nanofluid in rectangular ducts. Int J Therm Sci 172:107343

Kamsuwan C, Wang X, Piumsomboon P, Pratumwal Y, Otarawanna S, Chalermsinsuwan B (2023) Artificial neural network prediction models for nanofluid properties and their applications with heat exchanger design and rating simulation. Int J Therm Sci 184:107995

Li S, Zhou W, Sangani HA, Wang J, Wang J (2023) Optimization of heat transfer performance of a micro-bare-tube heat exchanger using a genetic algorithm. Energy Sci Eng 11(9):3164–3172

Liu Q, Tao Y, Shi L, Zhou T, Huang Y, Peng Y, Tu J (2023) Parametric optimization of a spiral ground heat exchanger by response surface methodology and multi-objective genetic algorithm. Appl Therm Eng 221:119824

Ma H, He B, Su L, He D (2023) Heat transfer enhancement of nanofluid flow at the entry region of microtubes. Int J Therm Sci 184:107944

Nazififard M, Nematollahi M, Jafarpur K, Suh KY (2012) Numerical simulation of water-based alumina nanofluid in subchannel geometry. Sci Technol Nucl Install 2012:1–12

Nguyen NP, Maghsoudi E, Roberts SN, Kwon B (2023) Shape optimization of pin fin array in a cooling channel using genetic algorithm and machine learning. Int J Heat Mass Transfer 202

Onyiriuka E (2023a) Predictive modelling of thermal conductivity in single-material nanofluids: a novel approach. Bull Natl Res Centre 47(1):140

Onyiriuka E (2023b) Predictive modelling of thermal conductivity in single-material nanofluids: a novel approach. Bull Natl Res Centre 47(1):139

Pan L, Yao Z, Yao W, Wei X (2023) Multi-objective optimization on bionic fractal structure for heat exchanging of two fluids by genetic algorithm. Int J Heat Mass Transfer 212:124298

Rudyak VY, Minakov AV (2018) Thermophysical properties of nanofluids. Eur Phys J E 41(1):15

Said Z, Sundar LS, Rezk H, Nassef AM, Ali HM, Sheikholeslami M (2021) Optimizing density, dynamic viscosity, thermal conductivity and specific heat of a hybrid nanofluid obtained experimentally via ANFIS-based model and modern optimization. J Mol Liquids 321:114287

Sridhara V, Satapathy LN (2011) Al 2 O 3-based nanofluids: a review. Nanoscale Res Lett 6:1–16

Usman MAA, Alghamdi M, Muhammad T (2022) A forced convection of water aluminum oxide nanofluid flow and heat transfer study for a three dimensional annular with inner rotated cylinder. Sci Rep 12(1):16735

Zhang T, Chen L, Wang J (2023) Multi-objective optimization of elliptical tube fin heat exchangers based on neural networks and genetic algorithm. Energy 269:126729

Publisher's Note